

## Porphyrin-POSS Molecular Hybrids

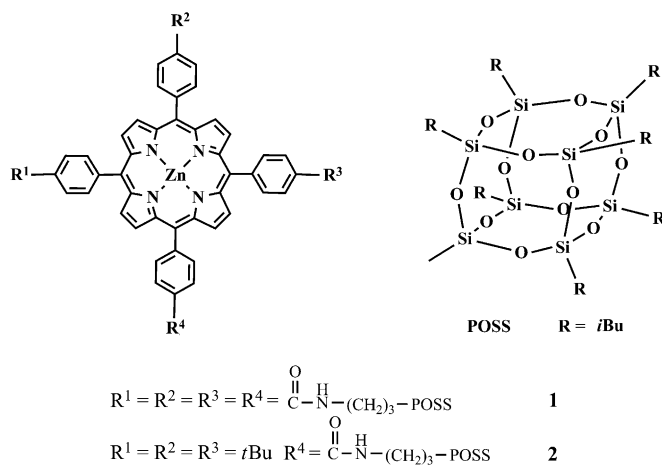
Junshan Sun,<sup>[a]</sup> Yanli Chen,<sup>[b]</sup> Luyang Zhao,<sup>[a]</sup> Yuting Chen,<sup>[a]</sup> Dongdong Qi,<sup>[a]</sup>  
Kyung-Min Choi,<sup>[c]</sup> Dong-Soo Shin,<sup>[c]</sup> and Jianzhuang Jiang\*<sup>[a]</sup>

Organic–inorganic hybrid materials have been a most effective source for advanced materials due to their wide range of applications associated with unique thermal, mechanical, rheological, chemical, and physical properties.<sup>[1–3]</sup> Starting from simply dispersing inorganic pigments or fillers into organic components for the purpose of yielding/improving functional and mechanical properties, different soft inorganic chemistry processes including sol-gel process, hydrothermal reaction, and self-assembly have been developed for incorporating functional organic and inorganic materials into organic–inorganic hybrid materials in a homogeneously dispersed manner.<sup>[4–6]</sup> However, despite the realization of combined inorganic and organic components at the nano-scale level,<sup>[7]</sup> truly homogenous dispersion of basic functional building blocks between organic and inorganic components for hybrid materials has not been achieved, thus far, due to the intrinsic differences in the nature of organic and inorganic interactions.<sup>[8]</sup> Fortunately, recent progress in organic–inorganic molecular hybrids has rendered homogenous dispersion of organic and inorganic functional building blocks at the molecular level.<sup>[9]</sup>

Among various inorganic building blocks, polyhedral oligomeric silsesquioxanes (POSS) are a new class of condensed three-dimensional oligomeric organosiliceous compounds with cage frameworks. They provide an excellent platform for the synthesis of organic–inorganic molecular hybrid materials<sup>[10]</sup> and have resulted in the recent preparation of quite a number of novel POSS-containing molecular hybrid materials including MCM-POSS,<sup>[11a]</sup> C<sub>60</sub>-POSS,<sup>[11b]</sup>

and graphene-POSS.<sup>[11c]</sup> However, POSS-containing molecular hybrid materials with porphyrin as organic component remain unknown. Due to the excellent photic, electric, and magnetic properties of these naturally occurring tetrapyrrole derivatives,<sup>[12,13]</sup> incorporation of porphyrins into molecular hybrids with the help of POSS is expected to yield corresponding materials with good properties, functionalities, and applications.

Herein, we describe the synthesis and spectroscopic characterization of two novel porphyrin–POSS molecular hybrid composites, namely [5,10,15,20-tetrakis((*N*-[heptakis(isobutyl)propyl]benzamidato)octasiloxane)phenyl]porphyrinato zinc [Zn{T(POSS)<sub>4</sub>PP}] (**1**) and [5-((*N*-[heptakis(isobutyl)propyl]benzamidato)phenyl)octasiloxane-10,15,20-tris(4-*tert*-butylphenyl)porphyrinato] zinc [Zn{M(POSS)PP}] (**2**; Scheme 1), as the first example of porphyrin–POSS mo-



Scheme 1. Schematic molecular structures of porphyrin–POSS hybrid compounds [Zn{T(POSS)<sub>4</sub>PP}] (**1**) and [Zn{M(POSS)PP}] (**2**).

lecular hybrids. Their organic–inorganic hybrid nature of the combined organic porphyrin chromophore and inorganic POSS moiety has been unambiguously revealed by single crystal X-ray diffraction analysis for both compounds. In particular, systematic and comparative studies of their electronic absorption and fluorescence spectroscopic properties clearly revealed the effects of the homogeneously dispersed POSS moieties covalently attached to the porphyrin periphery on porphyrin aggregation. The supramolecular interaction of the POSS moieties with other molecules demon-

[a] J. Sun, L. Zhao, Dr. Y. Chen, Dr. D. Qi, Prof. Dr. J. Jiang  
Beijing Key Laboratory for Science and Application of Functional  
Molecular and Crystalline Materials, Department of Chemistry  
University of Science and Technology Beijing  
Beijing 100083 (P. R. China)  
Fax: (+86) 10-6233-2462  
E-mail: jianzhuang@ustb.edu.cn

[b] Prof. Y. Chen  
Shandong Provincial Key Laboratory of  
Fluorine Chemistry and Chemical Materials  
School of Chemistry and Chemical Engineering  
University of Jinan, Jinan 250022 (P. R. China)

[c] K.-M. Choi, Prof. Dr. D.-S. Shin  
Department of Chemistry and Physics  
Changwon National University  
Changwon, GN, 641-773 (S. Korea)

Supporting information for this article is available on the WWW  
under <http://dx.doi.org/10.1002/chem.201301875>.

strates the advantage of combining organic and inorganic components at the molecular level in optimizing the optical properties of organic–inorganic hybrid materials.

Metal free 5,10,15,20-tetrakis(*p*-carboxylphenyl)porphyrin and 5-(*p*-carboxylphenyl)-10,15,20-tris(4-*tert*-butylphenyl)porphyrin together with their zinc complexes were prepared according to published procedures.<sup>[14]</sup> Chlorination of these two porphyrinato zinc compounds with SOCl<sub>2</sub> followed by treatment with aminopropylisobutyl-POSS afforded the target porphyrin–POSS molecular hybrids **1** and **2** (see the Experimental Section for details). Satisfactory elemental analysis results were obtained for these two newly prepared hybrid compounds **1** and **2** after repeated column chromatography followed by recrystallization. The hybrid nature of these two compounds was first revealed by MALDI-TOF mass spectroscopy (Figure S1 and Table S1 in the Supporting Information) and then by the well-resolved <sup>1</sup>H NMR spectroscopic results (Figure S2 and Table S2 in the Supporting Information). In the IR spectra of **1** and **2** (Figure S3 in the Supporting Information), the Si–O–Si stretching gives a very intense absorption around 1105 cm<sup>-1</sup> with the Si–C stretching at around 1250 cm<sup>-1</sup>.

Single crystals of the porphyrin–POSS molecular hybrid **2** suitable for X-ray diffraction analysis were obtained by slow diffusion of methanol into a solution of **2** in CHCl<sub>3</sub>. This compound crystallizes in the triclinic space group *P* $\bar{1}$  containing two molecules in each unit cell. As shown in Figure 1, the porphyrin–POSS hybrid nature of **2** has been

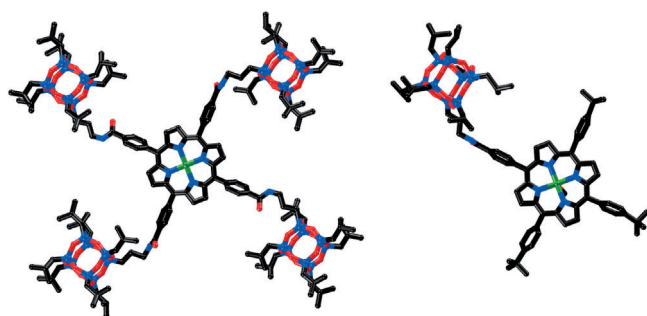


Figure 1. Molecular structures of [Zn{T(POSS)PP}] (**1**; left) and [Zn{M(POSS)PP}] (**2**; right) in top view. All hydrogen atoms and solvent molecules are omitted for clarity.

clearly revealed by single crystal X-ray diffraction analysis. One POSS cage is linked to the porphyrin core at one *meso*-attached phenyl moiety. For the porphyrin chromophore, the zinc ion locates in the center of porphyrin ring coordinated by four pyrrole N atoms and one O atom from a methanol molecule, forming a five-coordinate pentagonal pyramid geometry around the zinc ion. As a consequence, the porphyrin chromophore in **2** adopts a conformation that is slightly puckered. The zinc cation is displaced 0.238 Å from the N<sub>4</sub> plane. Nevertheless, two molecules of **2** are bound together through C–H⋯π stacking between the C–H bond of the phenyl moiety appended with the POSS group and a pyrrole π system of the second porphyrin ligand. The

distance from the H atom to the pyrrole center is 2.552 Å,<sup>[15]</sup> resulting in a dimeric supramolecular structure with porphyrin–porphyrin distance of 4.305 Å (Figure S4 in the Supporting Information). This basic building block further packs into a 1D chain through O⋯H–O hydrogen bonds formed between the carbonyl oxygen atom of the side chain of one dimer and the hydroxyl oxygen atom of the methanol coordinated with zinc ion of another dimer (Figure S4 in the Supporting Information). The O⋯O distance of 2.645 Å is comparable with those reported which fall in the range of 2.4–3.0 Å.<sup>[16]</sup>

Single crystals of **1** were also obtained by slow diffusion of MeOH into a CHCl<sub>3</sub> solution of this compound. Unfortunately, most probably because of the disorder in the four POSS moieties in the molecule, the quality of the crystals of **1** obtained was not good enough for X-ray diffraction analysis. The resulting data led to a relatively high R<sub>1</sub> value (0.18) even when the data were collected at 150 K. However, the hybrid nature of this compound with the porphyrin chromophore linked to four inorganic POSS cages through the four *meso*-phenyl moieties was unambiguously revealed on the basis of single crystal X-ray diffraction analysis (Figure 1). Similar to the analogue **2** with a single POSS cage appended, the zinc ion is also located in the center of porphyrin ring coordinated by four pyrrole N atoms and one O atom from a water molecule, showing a five-coordinated pentagonal pyramid coordination geometry for the zinc ion. The zinc cation is displaced 0.011 Å from the N<sub>4</sub> plane of porphyrin ring. In addition, the neighboring molecules of **1** are also bound together through O–H⋯O hydrogen bonds formed between the carbonyl oxygen atom of the side chain of one molecule and the oxygen atom of the water coordinated to the zinc ion of the second molecule with an O⋯O distance of 2.440 Å. C–H⋯π stacking between the C–H bond of the phenyl moiety and a pyrrole π system of the second porphyrin ligand with the distance from the H atom to the pyrrole center of 2.690 Å, forming a 1-D chain supramolecular structure with porphyrin–porphyrin distance of 4.842 Å are also observed (see Figure S4 in the Supporting Information).

It is well known that both phthalocyanine and porphyrin aggregate easily due to the effective π–π interaction between tetrapyrrole molecules with large conjugated electronic structures, resulting in corresponding oligomers and/or polymers in solution and self-assembled nano/microstructures in solid state.<sup>[17]</sup> Long range molecular ordering is certainly important for good performance of electronic devices. However, tetrapyrrole molecular aggregation was revealed to be detrimental for their optical application as exemplified in dye-sensitized solar cells (DSCs) due to the significantly decreased electron injection efficiency to conduction band of an inorganic semiconductor. To reveal the effect of covalently incorporated POSS moieties at the porphyrin periphery on the aggregation behavior, systematic investigation of the electronic absorption properties of both **1** and **2** in a wide range of concentrations in CHCl<sub>3</sub> was carried out. These data could be compared with those for [Zn-

(TBPP)] and the mixed samples of [Zn(TBPP)] and POSS in 1:1 and 1:4 ratios. As shown in Figure S5 and S6 (in the Supporting Information) and tabulated in Table S3 (in the Supporting Information), both the POSS appended porphyrinato zinc complexes display typical features of non-aggregated porphyrinato metal complexes in their electronic absorption spectra (recorded at concentrations as low as  $2.0 \times 10^{-6}$  M). An intense Soret band at around 420 nm and a relatively weak Q band at around 548 nm with a shoulder at 585 nm are observed similarly to their analogues including [Zn(TBPP)]. However, aggregation occurs with increasing the concentration. As shown in Figure S7 (in the Supporting Information), the molar extinction coefficients for **1**, **2**, [Zn(TBPP)], and the mixed samples of [Zn(TBPP)] and POSS in 1:1 and 1:4 ratios show obvious dependence on the concentration in a similar way. In the low concentration range the molar extinction coefficient remains almost unchanged until aggregation of the porphyrinato zinc molecules starts to occur. However, in comparison with [Zn(TBPP)], covalently introducing POSS moieties onto the porphyrin periphery in both **1** and **2** effectively prevents the Zn(Por) molecules from aggregating, leading to the aggregation starting at relatively higher concentration of approximately  $4.8 \times 10^{-6}$  and  $3.2 \times 10^{-6}$  M for **1** and **2**, respectively, relative to that of  $2.5 \times 10^{-6}$  M for [Zn(TBPP)] (Figure S7 in the Supporting Information). Interestingly, addition of either 1 or 4 equivalent amounts of POSS into the [Zn(TBPP)] CHCl<sub>3</sub> solution not only induces a small decrease in the molar extinction coefficient but fails to effect the aggregation behavior of the Zn(Por) chromophore in terms of the concentration at which aggregation starts to occur. These results clearly indicate the advantage of connecting organic and inorganic components at the molecular level in optimizing the aggregation and in turn the optical properties of organic-inorganic hybrid materials.

The fluorescence properties of **1** and **2** were comparatively studied with [Zn(TBPP)] as reference. Figures 2A and S8 (in the Supporting Information) show the fluorescence emission spectra of **1**, **2**, [Zn(TBPP)], and the mixed samples of [Zn(TBPP)] and POSS in 1:1 and 1:4 ratios (measured at the concentration of  $2.0 \times 10^{-6}$  M in CHCl<sub>3</sub> with the excited wavelength of 410 nm). As can be expected from the electronic absorption spectroscopic results detailed above, the fluorescence emission spectra of **1** and **2** are of very similar shape to that of [Zn(TBPP)] with a maximum emission band appearing at 601 nm and a shoulder at 644 nm. However, both the main emission band and the first shoulder in the fluorescence spectra of **1** and **2** are obviously more intense than those of [Zn(TBPP)], resulting in the higher fluorescence quantum yield of these two molecular hybrid materials (see Table S4 in the Supporting Information). This indicates the effective role of the covalently linked POSS moieties at the porphyrin periphery of **1** and **2** in preventing aggregation.<sup>[18]</sup> To provide more information in this regard, systematic studies of the relationship between the fluorescence quantum yield and concentration for all the five samples mentioned above, namely **1**, **2**, [Zn(TBPP)], and the

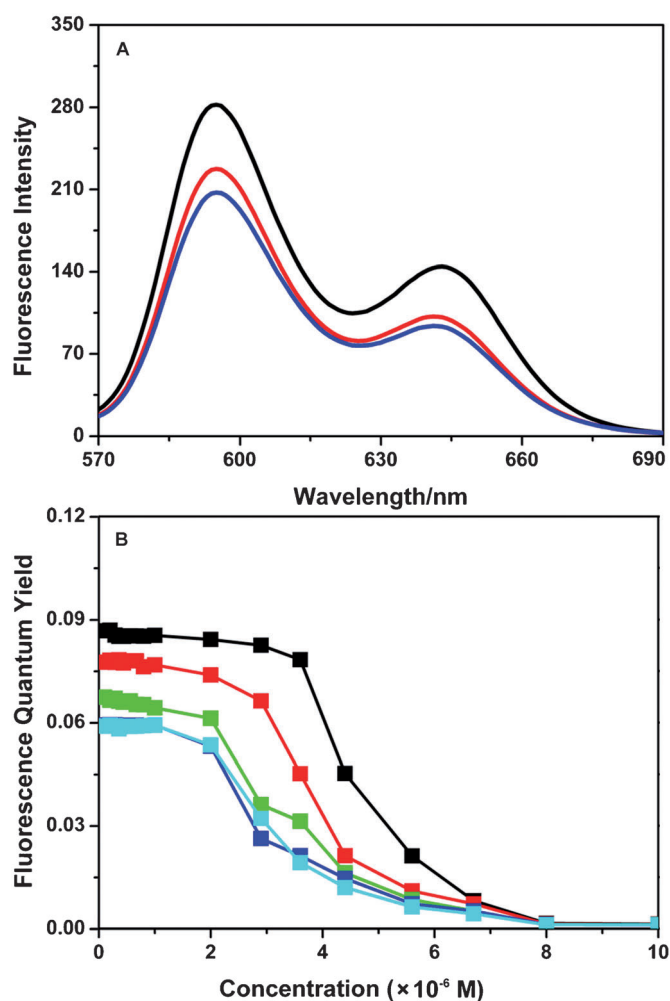


Figure 2. A) Fluorescence emission spectra of **1** (black), [Zn(TBPP)] (red), and the mixed samples of [Zn(TBPP)] and POSS in a 1:4 ratio (blue) at the concentration of  $2.0 \times 10^{-6}$  M in CHCl<sub>3</sub>. B) Plots of the fluorescence quantum yields for **1** (black), **2** (red), [Zn(TBPP)] (green), and the mixed samples of [Zn(TBPP)] and POSS in the ratio of 1:1 (blue) and 1:4 (turquoise; in terms of the porphyrinato zinc species) as a function of the concentration in the range of  $1.0 \times 10^{-7}$ – $1.0 \times 10^{-5}$  M with excitation at 410 nm. The fluorescence quantum yields were calculated with H<sub>2</sub>TBPP in chloroform (0.12) as reference.<sup>[19]</sup>

mixed samples of [Zn(TBPP)] and POSS in 1:1 and 1:4 ratios, in CHCl<sub>3</sub> with excitation at 410 nm were carried out. As shown in Figure 2B, the fluorescence quantum yields show a dependence on the concentration, which remains essentially unchanged in the low concentration range and then decreases significantly at the onset of aggregation. However, aggregation starts at a higher concentration for **1** and **2** (ca.  $3.6 \times 10^{-6}$  and  $2.9 \times 10^{-6}$  M, respectively), relative to that of [Zn(TBPP)] ( $2.0 \times 10^{-6}$  M; Figure 2B) confirming the effect of the POSS cages covalently linked at the porphyrin periphery in both **1** and **2** on preventing aggregation. This result is in agreement with that deduced from the electronic absorption measurements, as detailed above. Mixing the inorganic and organic components together by adding 1 or 4 equivalents of POSS into the [Zn(TBPP)] CHCl<sub>3</sub> solution

does not significantly change the concentration at which the aggregation begins, but induces a slight decrease in the fluorescence quantum yield of [Zn(TBPP)] (Figure 2B). As a consequence, covalently introducing POSS moieties onto the porphyrin periphery effectively optimizes the aggregation behavior and fluorescent properties of the porphyrin chromophore. This is in contrast to the slight negative effect revealed for mixing [Zn(TBPP)] and POSS (Table S4 in the Supporting Information).

To further clarify the effect of the POSS moieties covalently dispersed around the porphyrin periphery on the aggregation and photophysical properties of the porphyrin chromophore, the intermolecular fluorescence quenching of **1**, **2**, [Zn(TBPP)], and the mixed samples of [Zn(TBPP)] and POSS in 1:1 and 1:4 ratios by anthraquinone was comparatively investigated by spectroscopic titration methods. Interestingly, the electronic absorption spectrum of **1** ( $2.0 \times 10^{-6}$  M) undergoes a systematic change, in particular the porphyrin Soret band is red shifted from 421 to 448 nm upon titration with anthraquinone (from  $5.0 \times 10^{-5}$  to  $8.0 \times 10^{-4}$  M) recorded in  $\text{CHCl}_3$ , indicating the presence of significant ground state  $\pi$ - $\pi$  interactions between the Zn(Por) and anthraquinone chromophores (Figure 3A). This observation, in combination with the existence of several isosbestic points during the systematic change in the electronic absorption spectrum, reveals the formation of supramolecular structures with well-defined composition upon addition of anthraquinone. This seems to be related to the face-to-face Zn(Por)-anthraquinone hybrid dimer formed by the electronic interaction of the electron-rich Zn(Por) and electron-poor anthraquinone, as evidenced by the red-shift in the main electronic absorption bands of the porphyrinato zinc complex (Figure S9 in the Supporting Information).

NMR spectroscopic measurements also give good evidence for the  $\pi$ - $\pi$  interactions discussed above. As can be seen from Figures S10 and S11 (in the Supporting Information), addition of anthraquinone into a [Zn(TBPP)] solution in  $\text{CDCl}_3$  induces an upfield shift for the three sets of aromatic signals of [Zn(TBPP)], namely porphyrin pyrrole hydrogen and the two species of phenyl hydrogens, due to interaction of the aromatic ring current of anthraquinone with [Zn(TBPP)] in a face-to-face dimer.

To further clarify the formation of the face-to-face Zn(Por)-anthraquinone dimer in solution, theoretical calculations of the  $\pi$ - $\pi$  interaction between [Zn(TPP)] (TPP = dianion of tetra(phenyl)porphyrin) and anthraquinone on the basis of the optimized structure were conducted by DFT methods at the  $\omega\text{B97xd}$  level of theory.<sup>[20]</sup> The computational results reveal a high [Zn(TPP)]-anthraquinone  $\pi$ - $\pi$  interaction energy,<sup>[21]</sup>  $55.6 \text{ kcal mol}^{-1}$ , which seems to be responsible for the formation of the dimeric entity. Nevertheless, the red-shift observed for the Soret absorption band of Zn(Por) upon titration with anthraquinone is also well reproduced by the time-dependent DFT (TDDFT) calculations (Table S5 in the Supporting Information). This is also true for **2**, [Zn(TBPP)], and the mixed samples of [Zn(TBPP)] and POSS in 1:1 and 1:4 ratios (Figures S12–S15 in the Support-

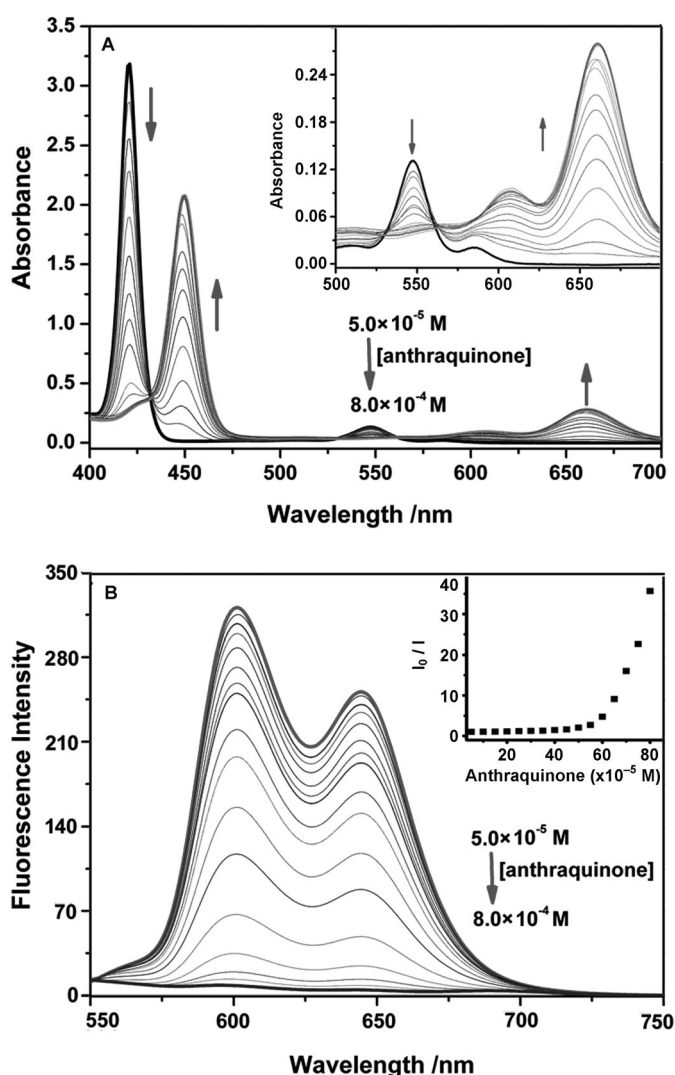


Figure 3. A) Electronic absorption and B) fluorescence emission spectra of **1** ( $2.0 \times 10^{-6}$  M) upon titration with anthraquinone (from  $5.0 \times 10^{-5}$  to  $8.0 \times 10^{-4}$  M) in  $\text{CHCl}_3$  with excitation at 410 nm. The inset shows the Stern–Volmer plot for the fluorescence quenching at 601 nm.

ing Information). In addition, the fluorescence emission bands of Zn(Por) for all these five samples at around 601 and 644 nm were found to diminish gradually during titration with anthraquinone in  $\text{CHCl}_3$  (Figures 3B and S16–S19 in the Supporting Information), due to the electron transfer from electron rich Zn(Por) to electron poor anthraquinone associated with the formation of a complex between the two species.<sup>[22]</sup> Comparison of the Stern–Volmer plots for the fluorescence quenching of **1**, **2**, [Zn(TBPP)], and the mixed samples of [Zn(TBPP)] and POSS in 1:1 and 1:4 ratios by anthraquinone (Figure S20 in the Supporting Information), confirms again the effect of covalently and homogeneously dispersed POSS moieties around the porphyrin periphery on the photophysical properties of Zn(Por). This is in contrast to the reverse effect observed when [Zn(TBPP)] and POSS are simply mixed together.

The association constants ( $K$ ) of Zn(Por) for **1**, **2**, [Zn(TBPP)], and the mixed samples of [Zn(TBPP)] and POSS in 1:1 and 1:4 ratios with anthraquinone were determined by the Benesi–Hildebrand equation ( $I_0/(I_0-I) = 1/A + 1/KA[\text{anthraquinone}]$ ), in which  $I_0$  and  $I$  represent the fluorescence intensity of Zn(Por) without and with the addition of anthraquinone, respectively, and  $A$  is a constant associated with the difference in the emission quantum yield of the complexed and uncomplexed Zn(Por).<sup>[23]</sup> By plotting  $I_0/(I_0-I)$  against  $1/[\text{anthraquinone}]$ , Figure 4, straight lines

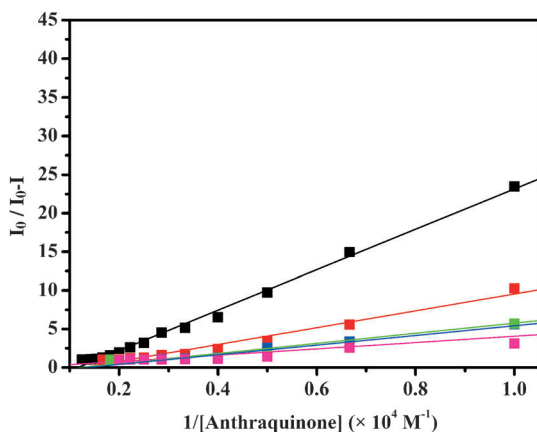


Figure 4. Benesi–Hildebrand plots for determining the association constants between anthraquinone and **1**, **2**, [Zn(TBPP)], or the mixed samples of [Zn(TBPP)] and POSS in the ratio of 1:1 and 1:4 ( $2.0 \times 10^{-6} \text{ M}$ ) by fluorescence titration in  $\text{CHCl}_3$ .

were obtained from which the values for  $K$  are determined ( $0.40$ ,  $0.90$ ,  $1.5$ ,  $1.6$ ,  $2.4 \times 10^3 \text{ M}^{-1}$  for **1**, **2**, [Zn(TBPP)], and the mixed samples of [Zn(TBPP)] and POSS in 1:1 and 1:4 ratios, respectively), indicating the increasing association tendency of Zn(Por) with anthraquinone. Nevertheless, the increase in the association constant along with this order gives additional support for the advantage of connecting the organic and inorganic components at the molecular level in optimizing the optical functional properties of hybrid materials.

In summary, two novel organic–inorganic molecular hybrid materials with porphyrin chromophores as the organic component and POSS as the inorganic part have been synthesized and structurally characterized. The aggregation/association behavior of the porphyrin chromophore has been revealed to be significantly optimized by the covalently and homogeneously dispersed POSS moieties around the porphyrin periphery. This in turn results in optimized electron absorption and fluorescence properties of porphyrin chromophores and should lead to improved functionality in DSCs and photo-catalysis. Nevertheless, the present result will also be helpful in the design and synthesis of general organic–inorganic hybrid materials with lower aggregation/association tendencies and therefore better properties and functionality.

## Experimental Section

**General:** The aminopropylisobutyl POSS was purchased from Hybrid Plastics (Hattiesburg, MS, USA). Tetrahydrofuran (THF) was freshly distilled from Na with diphenylketone under nitrogen atmosphere. Column chromatography was carried out on silica gel (Merck, Kieselgel 60, 70–230 mesh) with the indicated eluents. All other reagents and solvents were used as received. The compounds of metal free 5-(*p*-carboxylphenyl)-10,15,20-tris(4-*tert*-butylphenyl)porphyrin and 5,10,15,20-tetrakis(*p*-carboxylphenyl)porphyrin together with their zinc complexes were prepared according to the literature procedure.<sup>[14]</sup>

**Synthesis of [5-((*N*-heptakis(isobutyl)propyl)benzamidato)phenyl]octasiloxane-10,15,20-tris(4-*tert*-butylphenyl)porphyrinato zinc complex, [Zn(M(POSS)PP)] (**2**):** 5-(*p*-Carboxylphenyl)-10,15,20-tris(4-*tert*-butylphenyl)porphyrinato zinc (0.025 mmol) was added to thionyl chloride (20 mL) and refluxed under a slow stream of nitrogen for 3 h. The solvent was then removed under vacuum. Amino-propylisobutyl POSS (0.03 mmol) was dissolved in dry THF (30 mL) and then added into the reaction mixture in a dropwise manner over a period of 10 min. The resulting mixture was heated at  $80^\circ\text{C}$  for 2 h. The solvent was evaporated and the residue was chromatographed on a silica gel column by  $\text{CH}_2\text{Cl}_2/\text{petroleum ether}$  (2:1) as eluent. After evaporating the solvent under reduced pressure, the target compound **2** was obtained as a violet-red solid (83 %).

**Synthesis of [5,10,15,20-tetrakis((*N*-heptakis(isobutyl)propyl)benzamidato)octasiloxane]phenylporphyrinato zinc complex [Zn(T(POSS)PP)] (**1**):** By employing the above-described procedure with 5,10,15,20-tetra(*p*-carboxylphenyl)porphyrinato zinc instead of 5-(*p*-carboxylphenyl)-10,15,20-tris(4-*tert*-butylphenyl)porphyrinato zinc as starting material, **1** was isolated (85 %).

**Determination of the association constant of the Zn(Por)–anthraquinone dimer by fluorescence titration:** The concentration of **1**, **2**, [Zn(TBPP)] and the mixed samples of [Zn(TBPP)] and POSS in 1:1 and 1:4 ratios in  $\text{CHCl}_3$  was fixed at  $2.0 \times 10^{-6} \text{ M}$  and that for anthraquinone was changed from  $5.0 \times 10^{-5}$  to  $8.0 \times 10^{-4} \text{ M}$  with excitation at 410 nm (at which anthraquinone does not absorb light). The fluorescence due to the porphyrinato zinc compounds was observed. The absorbance values at the excitation wavelength were first normalized for all the samples before the fluorescence spectra were recorded. The absorbance values for all samples at the excitation wavelength were smaller than 0.1 to avoid reabsorption.

## Acknowledgements

Financial support from the National Key Basic Research Program of China (Grant Nos. 2013CB933402 and 2012CB224801), Natural Science Foundation of China, Beijing Municipal Commission of Education, and University of Science and Technology Beijing for JJ, and Korea Ministry of Environment (KME, 412–111–008) and National National Foundation of Korea (NRF-2010–0029634) for DS is gratefully acknowledged.

**Keywords:** fluorescence • molecular hybrid • porphyrin • polyhedral oligomeric silsesquioxanes • structure elucidation

- [1] V. M. Agranovich, Yu. N. Gartstein, M. Litinskaya, *Chem. Rev.* **2011**, *111*, 5179–5214.
- [2] R. P. Ortiz, A. Facchetti, T. J. Marks, *Chem. Rev.* **2010**, *110*, 205–239.
- [3] C. Sanchez, G. J. de A. A. Soler-Illia, F. Ribot, T. Lalot, C. R. Mayer, V. Cabuil, **2001**, *Chem. Mater.* **2001**, *13*, 3061–3083.
- [4] a) D. A. Loy, K. J. Shea, *Chem. Rev.* **1995**, *95*, 1431–1442; b) R. Ciriminna, M. Sciortino, G. Alonzo, A. D. Schrijver, M. Pagliaro, *Chem. Rev.* **2011**, *111*, 765–789; c) L. L. Hench, J. K. West, *Chem. Rev.* **1990**, *90*, 33–72; d) A. El Kadib, M. Bousmina, *Chem. Eur. J.* **2012**,

- 18, 8264–8277; e) M. Ozsoz, A. Erdem, D. Ozkan, K. Kerman, T. J. Pinnavaia, *Langmuir* **2003**, *19*, 4728–4732.
- [5] a) Q. Y. Yu, P. P. Wang, S. Hu, J. F. Hui, J. Zhuang, X. Wang, *Langmuir* **2011**, *27*, 7185–7191; b) R. C. Finn, J. Zubieta, *Inorg. Chem.* **2001**, *40*, 2466–2467; c) C. J. Warren, R. C. Haushalter, D. J. Rose, J. Zubieta, *Chem. Mater.* **1997**, *9*, 2694–2696; d) W. J. Chang, Y. C. Jiang, S. L. Wang, K. H. Li, *Inorg. Chem.* **2006**, *45*, 6586–6591; e) J. Liu, Q. Yang, L. Zhang, H. Yang, J. Gao, C. Li, *Chem. Mater.* **2008**, *20*, 4268–4275.
- [6] a) D. M. Vriezema, M. C. Aragonès, J. A. A. W. Elemans, J. J. L. M. Cornelissen, A. E. Rowan, R. J. M. Nolte, *Chem. Rev.* **2005**, *105*, 1445–1490; b) C. M. Drain, A. Varotto, I. Radivojevic, *Chem. Rev.* **2009**, *109*, 1630–1658; c) B. Dunn, J. I. Zink, *Acc. Chem. Res.* **2007**, *40*, 729–729; d) H. L. Zhai, W. G. Jiang, J. H. Tao, S. Y. Lin, X. B. Chu, X. R. Xu, R. K. Tang, *Adv. Mater.* **2010**, *22*, 3729–3734; e) A. X. Yin, Y. W. Zhang, C. H. Yan, *Chem. Eur. J.* **2011**, *17*, 8033–8038; f) U. Díaz, T. Garía, A. Veltý, A. Corma, *Chem. Eur. J.* **2012**, *18*, 8659–8672; g) L. Zhao, Z. Q. Lin, *Adv. Mater.* **2012**, *24*, 4353–4368.
- [7] a) Y. J. Kim, F. Zhao, M. Mitsuishi, A. Watanabe, T. Miyashita, *J. Am. Chem. Soc.* **2008**, *130*, 11848–11849; b) T. Ogoshi, Y. S. Chujo, *Macromolecules* **2003**, *36*, 654–660; c) Y. B. Guo, Q. X. Tang, H. B. Liu, Y. J. Zhang, Y. L. Li, W. P. Hu, S. Wang, D. B. Zhu, *J. Am. Chem. Soc.* **2008**, *130*, 9198–9199; d) T. S. Haddad, J. D. Lichtenhan, *Macromolecules* **1996**, *29*, 7302–7304; e) P. Maitra, J. Ding, H. Huang, S. L. Wunder, *Langmuir* **2003**, *19*, 8994–9004; f) J. G. Winiaz, L. M. Zhang, M. J. Lal, C. S. Friend, P. N. Prasad, *J. Am. Chem. Soc.* **1999**, *121*, 5287–5295; g) A. Pinna, C. Figus, B. Lasio, M. Piccinini, L. Malfatti, P. Innocenzi, *ACS Appl. Mater. Interfaces* **2012**, *4*, 3916–3922; h) F. B. Peng, L. Y. Lu, H. L. Sun, Y. Q. Wang, J. Q. Liu, Z. Y. Jiang, *Chem. Mater.* **2005**, *17*, 6790–6796.
- [8] M. B. Andrews, C. L. Cahill, *Chem. Rev.* **2013**, *113*, 1121–1136.
- [9] a) G. Bottari, G. D. L. Torre, D. M. Guldi, T. Torres, *Chem. Rev.* **2010**, *110*, 6768–6816; b) R. Otero, J. M. Gallego, A. L. V. Parga, N. Martín, *Adv. Mater.* **2011**, *23*, 5148–5176; c) V. K. Thakur, G. P. Ding, J. Ma, P. S. Lee, X. H. Lu, *Adv. Mater.* **2012**, *24*, 4071–4096; d) X. P. Sun, S. J. Dong, E. Wang, *J. Am. Chem. Soc.* **2005**, *127*, 13102–13103; e) J. J. Wang, Y. Q. Wang, F. F. Cao, Y. G. Guo, L. J. Wan, *J. Am. Chem. Soc.* **2010**, *132*, 12218–12221.
- [10] a) D. B. Cordes, P. D. Lickiss, F. Rataboul, *Chem. Rev.* **2010**, *110*, 2081–2173; b) D. B. Cordes, P. D. Lickiss, in *Advances in Silicon Science*, Vol. 3 (Ed.: C. Hartmann-Thompson), Springer, Heidelberg, **2011**, pp. 47–133.
- [11] a) K. S. Jang, H. J. Kim, J. R. Johnson, W. G. Kim, W. J. Koros, C. W. Jones, S. Nair, *Chem. Mater.* **2011**, *23*, 3025–3028; b) D. J. Clarke, J. G. Matison, G. P. Simon, M. Samoc, A. Samoc, *Appl. Organomet. Chem.* **2010**, *24*, 184–188; c) Y. H. Xue, Y. Liu, F. Lu, J. Qu, H. Chen, L. M. Dai, *J. Phys. Chem. Lett.* **2012**, *3*, 1607–1612.
- [12] *The Porphyrin Handbook*, Vols. 1–10 (Eds.: K. M. Kadish, K. M. Smith, R. Guilard), Academic Press, San Diego, **2000**; *The Porphyrin Handbook*, Vols. 11–20 (Eds.: K. M. Kadish, K. M. Smith, R. Guilard), Academic Press, San Diego, **2003**.
- [13] *Handbook of Porphyrin Science*, Vols. 1–15 (Eds.: K. M. Kadish, K. M. Smith, R. Guilard), World Scientific, Singapore, **2010**; *Handbook of Porphyrin Science*, Vols. 21–25 (Eds.: K. M. Kadish, K. M. Smith, R. Guilard), World Scientific, Singapore, **2012**.
- [14] Y. Chen, J. Jiang, *Org. Biomol. Chem.* **2012**, *10*, 4782–4787.
- [15] Y. Gao, X. Zhang, C. Ma, X. Li, J. Jiang, *J. Am. Chem. Soc.* **2008**, *130*, 17044–17052.
- [16] a) L. Sobczyk, S. J. Grabowski, T. M. Krygowski, *Chem. Rev.* **2005**, *105*, 3513–3560; b) A. Kollman, L. C. Allen, *Chem. Rev.* **1972**, *72*, 283–303.
- [17] a) *Phthalocyanine: Properties and Applications*, Vol. 1 (A. B. P. Lever, C. C. Leznoff), Wiley-VCH, New York, **1989**; *Phthalocyanine: Properties and Applications*, Vols. 2–3 (A. B. P. Lever, C. C. Leznoff), Wiley-VCH, New York, **1993**; *Phthalocyanine: Properties and Applications*, Vol. 4 (A. B. P. Lever, C. C. Leznoff), Wiley-VCH, New York, **1996**; b) H. Uno, A. Masumoto, N. Ono, *J. Am. Chem. Soc.* **2003**, *125*, 12082–12083.
- [18] G. Lu, Y. Chen, Y. Zhang, M. Bao, Y. Bian, X. Li, J. Jiang, *J. Am. Chem. Soc.* **2008**, *130*, 11623–11630.
- [19] X. Zhang, Y. Li, D. Qi, J. Jiang, X. Yan, Y. Bian, *J. Phys. Chem. B.* **2010**, *114*, 13143–13151.
- [20] J. D. Chai, M. Head-Gordon, *Phys. Chem. Chem. Phys.* **2008**, *10*, 6615–6620.
- [21] K. Wang, D. Qi, H. Wang, W. Cao, W. Li, J. Jiang, *Chem. Eur. J.* **2012**, *18*, 15948–15952.
- [22] C. S. Rajesh, G. J. Capitosti, S. J. Cramer, D. A. Modarelli, *J. Phys. Chem. B.* **2001**, *105*, 10175–10188.
- [23] X. Li, D. K. P. Ng, *Eur. J. Inorg. Chem.* **2000**, 1845–1848.

Received: May 15, 2013  
Published online: August 26, 2013